Anal. Chem. **2007,** *79,* 5264−5271

Detection of Separated Analytes in Subnanoliter Volumes Using Coaxial Thermal Lensing

Fuping Li,[†] Alexander A. Kachanov,[†,‡] and Richard N. Zare*,[†]

Department of Chemistry, Stanford University, Stanford, California 94305-5080, and Skymoon Research and Development, 3671 Enochs Street, Santa Clara, California 95051

A collinear-beam thermal lens detector has been constructed and its properties were characterized. Its application to the high-performance liquid chromatography (HPLC) separation of a mixture of five anthraquinone dyes dissolved in water shows a linear response over 3.5 orders of magnitude and a detection limit that is subnanomolar in the dye concentrations. These results are compared with those obtained previously using cavity ring-down spectroscopy (CRDS) in a Brewster's angle flow cell (Bechtel, K. L.; Zare, R. N.; Kachanov, A. A.; Sanders, S. S.; Paldus, B. A. *Anal. Chem.* 2005, 77, 1177−1182). The peak-to-peak baseline noise of the thermal lensing detection is 3.5×10^{-8} absorbance units (AU) with a path length of 200 μm, whereas the peak-to-peak baseline noise of CRDS detection is $\sim 2 \times 10^{-7}$ AU with a path length of 300 μm. Both of these figures of merit should be compared to the peak-to-peak baseline noise of one of the best commercial UV−vis HPLC detection systems, which is $\sim 5 \times 10^{-6}$ AU with a path length of 10 mm (1-s integration time). Therefore, the thermal lensing technique has a demonstrated sensitivity of subnanomolar detection that is ~140 times better than that of the best commercial UV−vis detector and ~5 times better than that of CRDS.

UV−vis absorption is one of the most widely employed detection schemes for high-performance liquid chromatography (HPLC). One particular advantage of UV−vis absorption detection is that the data are readily interpreted using the Beer−Lambert law, which gives directly the concentration c of the sample from measured absorbance $A = c\epsilon L$ provided that we know the sample extinction ϵ and path length L. Absorption detection is widely applicable because almost all organic compounds absorb in the visible or UV ranges of the spectrum. Its sensitivity may turn out to be insufficient, however, if either ϵ or L is too small. For the best commercial UV−vis detectors, the limit of detection (LOD) is on the order of 10^{-5} absorbance units (AU) for a 10-mm path length. Such a LOD means that the smallest detectable relative change in transmitted intensity caused by the presence of an analyte peak at the exit of a separation column is 2.3×10^{-5} or 23 parts per million (ppm). For an analyte with molar extinction $\epsilon = 2.3 \times 10^3$ cm^{-1}/M, this results in a minimum detectable concentration of 10 nM.

For many purposes, this performance is quite satisfactory. However, most recent HPLC systems use columns with internal diameters as small as 0.3 mm and injection volumes of ~30 nL. The entire separation cycle in such systems may take less than 1 min, resulting in peak widths of fractions of a second. As a result, traditional microliter-volume UV−vis absorption cells are not applicable. Devices that use capillary or microchannel separations also require much smaller sample volumes. This makes increasingly evident the need to develop more sensitive absorption detection systems with rapid response, very small sample volumes, and absorption path lengths.

An ideal absorbance detection method capable of working with very short absorption path lengths with limits of detection of analytes comparable to existing methods should have increased sensitivity inversely proportional to the absorption path length. For a 0.3-mm-long absorption cell, the sensitivity should be 33 times better than was necessary with a traditional 10-mm-long cell. This requires a LOD of 3×10^{-7} AU or 0.7 ppm in transmission, which cannot be achieved by classical UV−vis absorption.

One possible approach is to arrange an optical cavity around the flow cell. The optical absorption signal will then be enhanced due to multiple passages of the optical radiation within the cavity. In one such cavity-enhanced method, called cavity ring-down spectroscopy (CRDS), optical loss in the cavity can be determined very precisely by measurement of the decay time of the optical radiation injected into the cavity. A significant improvement in LOD has been achieved already in the first attempts with a pulsed laser,[1,2] when a liquid flow cell was inserted into a cavity formed by two very high reflectivity mirrors (supermirrors). Recently Bechtel and co-workers[3] further reduced noise by using a very compact semiconductor-based continuous-wave laser and the same improved Brewster's angle cell as in ref 2. They achieved a LOD of 2×10^{-7} AU and a dynamic range of 2.5 orders of magnitude on an absorption path length of 0.3 mm. This was a 50-fold improvement over conventional UV−vis HPLC, and it demonstrated that optical absorption detection in HPLC with very short absorption paths can be a reality. Such a LOD in absorbance corresponds to a detection limit of 7.3 nM for a medium with a molar extinction $\epsilon = 10^4$, such as, for example, quinalizarin dye

* To whom correspondence should be addressed. E-mail: zare@stanford.edu.
[†] Stanford University.
[‡] Skymoon Research and Development.

(1) Xu, S.; Sha, G.; Xie, J. *Rev. Sci. Instrum.* **2002**, *73*, 255−258.
(2) Snyder, K. L.; Zare, R. N. *Anal. Chem.* **2003**, *75*, 3086−3091.
(3) Bechtel, K. L.; Zare, R. N.; Kachanov, A. A.; Sanders, S. S.; Paldus, B. A. *Anal. Chem.* **2005**, *77*, 1177−1182.

10.1021/ac0705925 CCC: $37.00
Published on Web 06/15/2007

at 488 nm. This is even slightly better than the limit of detection of a conventional UV−vis detector of 11 nM.

The CRDS approach to HPLC detection still needed improvement because rather long (tens of centimeters) cavities were used in the first experiments.[2,3] Moreover, cell diameters of a few millimeters were required in order to reduce diffraction losses. This means that the absorption cell has a volume of 2−6 μL even with a submillimeter cell length. There also exist two difficulties associated with using an intracavity Brewster's angle cell. The first is internal stress in fused-silica cell windows. It is always present, even with good annealing. Depolarization of light within the cavity from such stress breaks the Brewster's condition and makes it difficult to achieve an insertion loss of the cell smaller than several hundred ppm. The second problem involves reflection losses on the glass−liquid interface arising from fluctuations in the liquid refractive index.

Making a small (2 mm long) CRDS cavity with the mirrors in direct contact with the liquid mobile phase[4−6] solves the problems of beam diameter and polarization loss discussed above, but it brings up a new one—the cavity decay time is too short and difficult to measure. For this reason, in the first "wet mirror" experiment,[4] the LOD was only 2.7×10^{-5} AU. In an improved version,[5] the LOD has been decreased 10 times, reaching the value of 2.7×10^{-6} AU, which is 13 times worse than the best result achieved with an intracavity flow cell.[3] The difficulty of achieving sufficiently long decay times increases as the wavelength is shortened. Indeed, in an experiment with UV excitation,[6] the same group could only achieve a LOD of 2.7×10^{-5} AU, which is comparable with conventional UV−vis detection. Also, the cell volume in these experiments was close to 12 μL, which is too large for micro-HPLC and nano-HPLC applications.

In a different method of cavity-enhanced absorption,[7] a small wet mirrors cavity was locked to a narrow linewidth laser, and the enhanced absorption was determined by measuring the optical power reflected from the cavity. This method is potentially capable of achieving a photodetector shot noise limited sensitivity that is equivalent to a LOD of 1.5×10^{-8} AU, even though the LOD demonstrated in the first experiment was only 8×10^{-7} AU.

In summary, all methods using cavities have a common problem in their application for low-volume separation analytical technologies. The majority of analytes have noticeable absorption only in the UV or even deep UV region of the spectrum. It becomes increasingly difficult to make highly reflecting mirrors in this range. Moreover, high intensities circulating in the high-finesse cavities may cause mirror degradation in the deep UV range. Finally, the mobile-phase constituents, such as methanol, may themselves have a rather high UV absorption, which limits the number of round trips in the cavities and thus reduces the advantage of using cavities for absorption measurements of this type.

As an alternative approach to cavity-enhanced technologies, a large variety of photothermal methods promise to be much more suitable for ultrasensitive measurements of optical absorption in very small volumes. They all rely on a local change of the refractive index induced by local heating that results from optical absorption of a laser beam (excitation beam) focused within this small volume. If another optical beam is sent through a perturbed area, the local refractive index perturbation will act on the wave front of the probe beam as a negative lens, and it will increase the probe beam divergence as shown schematically in Figure 1. The increased divergence will result in a decrease of probe beam intensity on the beam axis ΔI, which can be measured with a photodetector placed behind a small aperture on the beam axis. This technique, called thermal lensing (TL), has been known since the mid-1960s—nearly as long as lasers have existed. Excellent reviews of the TL, including its elementary theory, are available,[8−11] and various applications of this technique have been demonstrated, including measurements directly in capillaries[12−16] and microchips.[17] For strongly absorbing nonfluorescing dyes, the detection of single[18] and subsingle[19] molecules in a very small probe volume within the liquid has been reported.

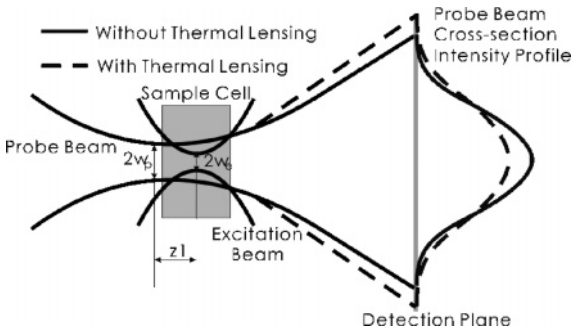

Figure 1. Excitation and probe beam arrangement for coaxial thermal lensing.

The measurement of a relative change in the probe beam intensity $\Delta I/I_0$ induced by absorption of an intensity chopped excitation beam is very similar to the measurement of the relative intensity change $\Delta I/I_0$ in traditional UV−vis spectroscopy. One important benefit of TL is that for a high-power excitation beam this relative change of the probe beam can be much larger than that from direct absorption. This is often referred to as the "thermal lens enhancement factor". In water with a He−Ne laser as a probe source, the thermal lens enhancement factor is equal to one for an excitation beam power of only 4.3 mW. An even

(4) Bahnev, B.; van der Sneppen, L.; Wiskerke A. E.; Ariese, F.; Gooijer, C.; Ubachs, W. *Anal. Chem.* **2005**, *77*, 1188−1191.
(5) van der Sneppen, L.; Wiskerke, A.; Ariese, F.; Gooijer, C.; Ubachs, W. *Anal. Chim. Acta* **2006**, *558*, 2−6.
(6) van der Sneppen, L.; Wiskerke, A.; Ariese, F.; Gooijer, C.; Ubachs, W. *Appl. Spectrosc.* **2006**, *60*, 931−935.
(7) McGarvey, T.; Conjusteau, A.; Mabuchi, H. *Opt. Express* **2006**, *14*, 10441−10451.
(8) Fang, H. L.; Swofford, R. L. In *Ultrasensitive Laser Spectroscopy*; Kliger, D. S., Ed.; Academic Press: New York, 1983.
(9) Dovichi, N. J. *Prog. Anal. Spectrosc.* **1988**, *11*, 179−207.
(10) Bialkowski, S. E. In *Photothermal Spectroscopy Methods for Chemical Analysis*; Winefordner, J. D., Ed.; Chemical Analysis 134; Wiley: New York, 1996.
(11) Abbas, K.; Ghaleb, J.; Georges, J. *Spectrochem. Acta A* **2004**, *60*, 2793−2801.
(12) Yu, M.; Dovichi, N. J. *Anal. Chem.* **1989**, *61*, 37−40.
(13) Bruno, A. E.; Paulus, A.; Bornhop, D. *J. Appl. Spectrosc.* **1991**, *45*, 462−467.
(14) Waldron, K. C.; Dovichi, N. J. *Anal. Chem.* **1992**, *64*, 1396−1399.
(15) Waldron, K. C.; Li, J. *J. Chromatogr., B* **1996**, *683*, 47−54.
(16) Qi, M.; Li, X.-F.; Stathakis, C.; Dovichi, N. J. *J. Chromatogr., A* **1999**, *853*, 131−140.
(17) Sato, K.; Kawanishi, H.; Tokeshi, M.; Kitamori, T.; Sawada, T. *Anal. Sci.* **1999**, *15*, 525−529.
(18) Tokeshi, M.; Uchida, M.; Uchiyana, K.; Sawada, T.; Kitamori, T. *J. Lumin.* **1999**, *83*, 261−264.
(19) Tokeshi, M.; Uchida, M.; Hibara, A.; Sawada, T.; Kitamori, T. *Anal. Chem.* **2001**, *73*, 2112−2116.

more important advantage is that a very low noise laser can be used for the probe beam. Then a LOD close to the probe beam photocurrent shot noise level can be reached with a lock-in detector. In TL, we substitute the measurement of a small-intensity change of the excitation beam on the high-intensity background by the measurement of the probe beam modulation on zero background. As an example, for a He−Ne laser with only 1 mW optical power, a shot noise limited relative intensity change of 2.7×10^{-8} can be measured with a 1-s averaging time. Assuming an excitation laser power of 4.2 mW and thus no thermal lens enhancement, this is equivalent to a LOD of 1.2×10^{-8} AU—more than a 10-fold improvement over the best result achieved with CRDS.

All this makes TL appear to be an ideal candidate for an optical detector with sensitivity comparable to or even higher than that of traditional UV−vis detection in ultrasmall absorption cells compatible with micro- or nano-HPLC, or with a capillary in capillary-format separations. By tightly focusing the excitation beam, TL should be able to measure absorption directly within the liquid sample. The influence of the cell windows' absorption will then be significantly reduced—a very important advantage for detection in the deep UV. In addition, TL is far less sensitive to the solvent absorption than are cavity-enhanced methods. Finally, TL does not require the excitation beam to be a laser beam, and indeed, a TL detector with a light-emitting diode has already been demonstrated.[20]

THE PURPOSE OF THIS WORK

In our opinion, one of the factors that limits the applications of TL for micro- and nanovolume analytical technologies is the research community's lack of awareness of how important experimental parameters, such as the size of the excitation and probe beams and their spatial mismatch, affect the response of the detector, the detection limits, and the stability and reproducibility of the measurements. To a great extent, this situation arises from the fact that this information cannot be expressed by simple analytical formulas, in contrast to traditional TL where such design guidelines and simple-to-use equations have been derived.[21,22] The complexity comes from the fact that small-volume TL measurement implies strongly focused beams. Then the cross section of the excitation beam and consequently of the thermally perturbed area within the sample is no longer constant along the sample axis. The extent of the beam size variation can be determined by comparing the sample thickness with the Rayleigh range $Z_R = (1/2)kw_0^2$ of the beam, where k is the probe beam wave vector in the medium and w_0 is its Gaussian waist size. The beam size w depends on the distance z from the waist as $w(z)^2 = w_0^2(1 + (z/Z_R)^2)$. From this it is clear that the domain in z within $\pm Z_R$ corresponds to high absorbed energy density and strong thermal lensing because at $z = Z_R$ the beam area is only twice as big as it is at the waist position. For example, in the single-molecule detection experiment of Tokeshi et al.,[19] with $Z_R = 4.7$ μm, the diameter of the excitation beam is only 1.6 μm in the middle of their 100-μm-long cell, but its size at the cell entrance and exit planes is 14.9 μm.

(20) Malik, A. K.; Faubel, W. *Chem. Soc. Rev.* **2000**, *29*, 275−282.
(21) Sheldon, S.; Knight, L.; Thorne J. *Appl. Opt.* **1982**, *21*, 1663−1669.
(22) Shen, J.; Lowe, D.; Snook, R. *Chem. Phys.* **1992**, *165*, 385−396.

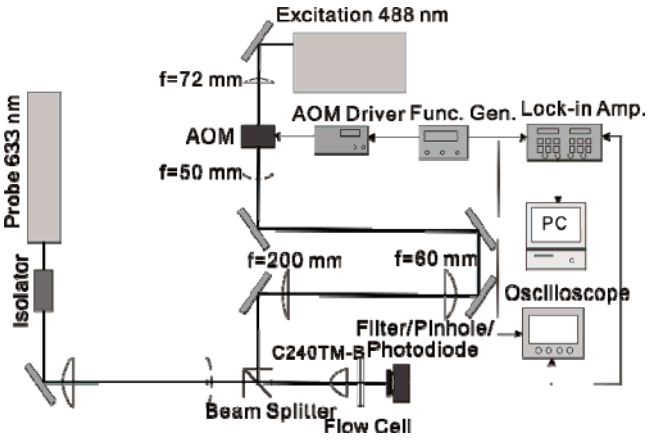

Figure 2. Experimental setup for the measurement of beam properties of the excitation beam (blue) and the probe beam (red).

In this and similar experiments with tight focusing, the beam interaction area changes dramatically along the cell, and only numerical beam propagation methods can help in modeling the detector response. Worse, the tightly focused beams have high numerical aperture (NA) and often focusing reduces beam quality (represented by their M^2 value[23]), causing there to be a larger multidimensional space of important experimental parameters that needs to be explored.

In this paper, we are presenting a design of an ultrasensitive collinear TL measurement system for HPLC and an experimental study of the influence of experimental parameters such as the degree of focusing and waist position mismatch on its response, as well as the impact of these parameter variations on its stability and reproducibility. We verify how far the experimental results with tightly focused beams can be from the predictions of "thin lens" theory and how local such measurements are. To determine calibration factors and the LOD in absorbance units and in concentration for an optimized TL detector, we use chromatographic separation results obtained previously for the same absorption cell, the same mixture of analytes, and the same light source with a different method that gives exact absorbance values (CRDS).

EXPERIMENTAL SECTION

We have chosen a coaxial TL detection configuration for the sake of simpler alignment and easier control. We were also encouraged by single-molecule detection reports[17−19] that used this configuration. This study concentrates on the effects of the probe beam waist size and the position mismatch between the excitation beam waist and the probe beam waist.

Figure 1 shows the scheme for the coaxial TL study. As shown in the figure, w_e and w_p are the waist sizes of the excitation beam and the probe beam, respectively, and $z1$ denotes the distance between the foci of the two beams. The change of the probe beam divergence due to TL is shown by a dotted line. We wished to find the combination of w_p and $z1$ that for a given w_e produces the maximum relative change of intensity at the probe beam axis, and therefore, we designed our setup so that it can be configured both for beam parameter measurement (Figure 2) and for TL detection (Figure 3).

The probe beam source was a low-noise, 2-mW He−Ne laser (model 1122, JDS Uniphase, Milpitas, CA) operating at the

(23) Siegman, A. E. *Proc. SPIE* **1990**, *1224*, 2−14.

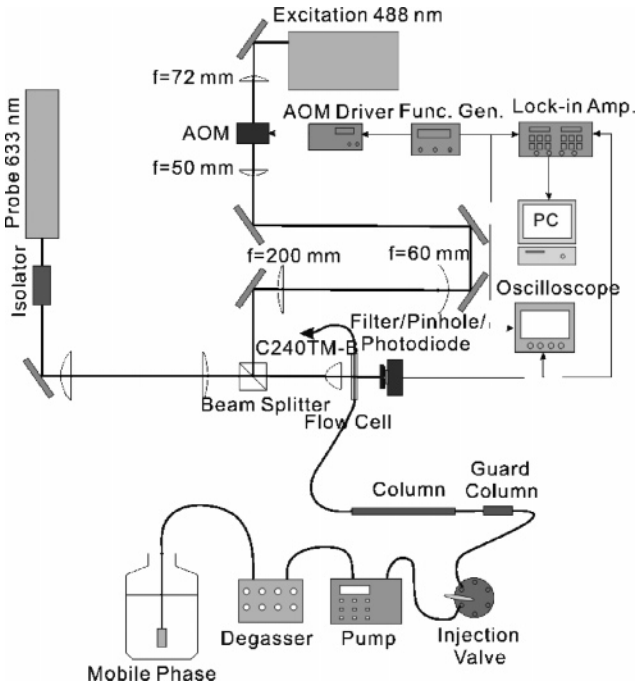

Figure 3. Experimental setup for HPLC thermal lensing detection.

wavelength λ_p = 633 nm, with output beam diameter and divergence angle at $1/e^2$ level of 0.63 mm and 1.3 mrad, respectively. A telescope formed by two plano-convex lenses was inserted into the probe beam so that its beam size and position within the flow cell could be changed by using different lens sets with different focal lengths in the telescope. An optical isolator (model IO-3-650-LP, Optics for Research, Caldwell, NJ) was placed between the laser and the telescope to prevent the reflected beam from re-entering the laser and destabilizing it. The isolator, initially designed for operation at 650 nm, was readjusted in order to provide good optical isolation at the probe beam wavelength.

The excitation beam source, with output power of 40 mW at the wavelength λ_e = 488 nm, output beam diameter and divergence angle at $1/e^2$ level of 0.70 mm and 1.1 mrad, respectively, and beam quality parameter $M^2 < 1.1$, was custom-made by Picarro, Inc. (Sunnyvale, CA), and it was the same as the one used elsewhere.[3] The 488-nm beam was focused by a lens with focal length f = 72 mm into an acousto-optic modulator (AOM) (model TEM-85-10, Brimrose, Baltimore, MD) so that its diffracted beam formed the excitation beam modulated in intensity without introduction of any mechanical perturbation to the setup. The modulation frequency of the excitation beam (1050 Hz) was controlled by a function generator (model 8116A, HP, Palo Alto, CA). The diffracted excitation beam was collimated with an f = 50 mm lens followed by a telescope formed by a pair of lenses with focal lengths f = 60 mm and f = 200 mm, respectively.

The vertically polarized probe beam and horizontally polarized excitation beam were combined by a polarizing beam splitter and then they shared a common path. Both beams were focused into a flow cell by an aspheric lens with focal length f = 8 mm and numeric aperture NA = 0.5 (model C240TM-B, Thorlabs, Newton, NJ).

In all experiments, we used the same five dyes of the anthraquinone family as in a previous study.[3] All dyes were purchased from Sigma-Aldrich (St. Louis, MO) and used as received. We also used the same solvent as described in the HPLC section.

A. Measurement of the Beam Properties. In the first step, the spot size and position for the excitation beam as well as spot sizes and positions of the probe beam relative to the excitation spot for different telescope magnifications were measured using the setup in Figure 2. Two beams were focused by the aspheric lens into a fused-silica flow cell (model 48UV0.1, NSG Precision Cells, Inc., Farmingdale, NY). The cell had a liquid layer thickness of 0.1 mm, window thickness of 1.25 mm, and volume of 30 μL.

The beam in the cell was reimaged by a Zeiss Achroplan ×20 microscope objective lens and an f = 250 achromatic doublet lens arranged confocally so that they formed a 31.25 times enlarged image of the beam waist in the cell in the back focal plane of the lens. A Thorlabs rotating blade beam profiler (model WM100) was placed in the back focal plane of the lens. This arrangement not only gave access to the waist within the flow cell but also brought its size into the measurement range of the beam profiler. In addition, the Zeiss objective has a glass thickness compensation collar, providing aberration-free imaging of the beam waists in the middle of the cell. The objective was mounted on a precise translation stage with a stepper motor actuator providing submicrometer resolution. This allowed us first to find the excitation beam size and position and then to determine in the same coordinate system the locations and sizes of the probe beam for different probe beam telescope magnifications. The telescope also was very helpful in precise coaxial alignment of the probe beam versus the excitation beam. When the excitation beam was measured, the AOM was constantly turned on.

For the beam characterization, the signal from the beam profiler was collected and digitized by a 500-MHz oscilloscope (model LT342, LeCroy, Chestnut Ridge, NY) connected to a personal computer via GPIB interface. The profiles at different positions around focus were analyzed by a LabView program and fitted to theoretical dependence to give the beam waist size, position, and M^2 of the beam. The waist sizes and positions obtained in this manner were used in the second step for TL signal parametric study, and optimization. We used the same solvent for the beam characterization as for the TL optimization and for HPLC measurements in order to make the results comparable. More experimental details can be found in F.L.'s Ph.D. thesis.[24]

B. Thermal Lensing Response Optimization. In the second step, the response of our photothermal detector was recorded as a function of the previously measured size and position of the probe beam spot using a constant flow of 5 μM quinizarin at a rate of 5 mL/h provided by a syringe infusion pump. The constant flow is important because a static solution would become bleached under the illumination of the strongly focused excitation beam and would result in an unstable signal. Quinizarin dye was chosen as the sample test solution because of its high molar extinction coefficient (ϵ = 7.3 × 10^3 M^{-1} cm^{-1}) and its relatively high solubility in water (0.2 mg/mL). The beam power after the focusing lens and before the flow cell was ~28 mW for the excitation beam and 1.7 mW for the probe beam. At this step, the beam profiler was replaced by an amplified silicon photodetector

(24) Fuping Li, Ph.D. thesis, Thermal Lensing and Its Applications to Liquid Chromatography. Stanford University, Stanford, CA, 2006.

(model PDA55, Thorlabs) as shown in Figure 3. A pinhole was placed before the photodiode to sample probe beam intensity on axis. A 10-nm bandpass filter centered at 633 nm was inserted in front of the photodiode in order to block the excitation beam at 488 nm and most of the ambient light. The whole photodiode assembly was mounted on an XY-stage in order to align the pinhole with the probe beam axis. The photodiode was placed in the far field zone—more than 150 Rayleigh lengths z_R away from the waist position of the probe beam. At this stage, the pump beam was modulated by the AOM at a frequency of 1050 Hz.

For quantitative measurements, we used a lock-in amplifier (model SR830, Stanford Research Systems, Sunnyvale, CA), which we controlled with a LabView program via GPIB. The time constant of the lock-in amplifier was set at 1 s; the low-pass filter slope was 24 dB/octave, which resulted in the equivalent noise bandwidth of 0.078 Hz. In all TL measurements, we intentionally set the photodetector gain such that the constant components of the probe beam photocurrent I_0 were close to 10 V in order to minimize the contribution of the detector's own noise to the TL signal $\Delta I/I_0$, where ΔI is the photocurrent variation caused by the thermal lens. The transimpedance gain of the photodetector in all measurements was 4.7×10^5 V/A.

C. HPLC Detection. To enable a direct comparison of detection sensitivity between the previous CRDS study[3] and TL, the same five anthraquinone dyes were chosen for HPLC detection: alizarin (1,2-dihydroxyanthraquinone), purpurin (1,2,4-trihydroxyanthraquinone), quinalizarin (1,2,5,8-tetrahydroxyanthraquinone), emodin (6-methyl-1,3,8-trihydroxyanthraquinone), and quinizarin (1,4-dihydroxyanthraquinone). The same separation scheme as before was chosen for these five compounds. We used an isocratic separation scheme and the mobile phase composed of 80% HPLC grade methanol (Fisher Scientific, Pittsburgh, PA) and 20% deionized water (18.2 MΩ × cm, Millipore, Billerica, MA) to which 5% glacial acetic acid (99.9%, Baker, Phillipsburg, NJ) was added (pH 3.6). The HPLC system in the setup consisted of a mobile-phase reservoir, a degasser (model 3014A, Waters, Milford, MA), a dual-piston pump (model LC-10AD$_{vp}$, Shimadzu, Kyoto, Japan), an injection valve (model 02W-010H, Valco Cheminert, Gig Harbor, WA), a guard column, and a HPLC column (model Zorbax Eclipse XDB-C18, Agilent, Santa Clara, CA). The HPLC column was packed with 5-μm end-capped C_{18} particles, and the column was 150 mm long with an inner diameter of 4.6 mm. A 1 mL/min pump rate was employed in the experiment. The sample injection loop volume was 20 μL. The eluate exiting from the HPLC column was connected to the flow cell in the TL detection system.

The experimental setup of the TL system shown in Figure 3 was practically the same as the one used for TL detection optimization with the following minor modifications: The probe laser used in HPLC detection was a 2-mW frequency and intensity stabilized HeNe laser (model 117A, Newport, Irvine, CA). For the purpose of direct comparison, the flow cell was replaced by a 200-μm path length, 10-μL flow cell that was used previously.[3] The aspheric focusing lens was replaced by the Zeiss Achroplan ×20 microscope objective lens that has the same NA and focal length. The excitation beam and the probe beam shared a common ×4 telescope composed of two plano-convex BK-7 lenses with focal lengths of 15 and 60 mm. Other experimental conditions remained the same. The excitation beam modulation frequency was changed to 1400 Hz, which provided the best signal-to-noise ratio.

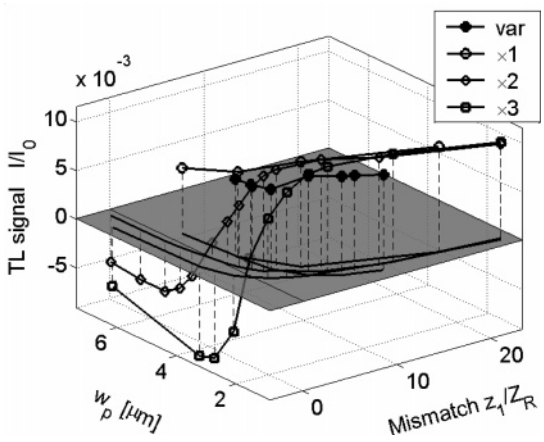

Figure 4. Combined results of all measurements of TL response for 5 μM quinizarin solution as a function of probe beam waist sizes versus telescope magnification (a), and (b).

RESULTS

A. Optimum Probe Beam Settings. The excitation beam was initially focused in the middle of the liquid layer in the flow cell, and it was unchanged through the entire set of experiments. We found its beam waist w_e to be 1.2 μm; the measured M^2 value of 1.6 was somewhat worse than the initial $M^2 = 1.1$ owing to aberrations in the cell window (the aspheric lens did not compensate for the cell window thickness). This larger M^2 value was not a problem because all we needed from the excitation beam was for it to be tightly focused into the liquid layer. We also needed its size dependence on the propagation coordinate, which can be determined from the beam propagation law for nonideal Gaussian beams.[23] Then we measured TL signals for a large variety of the probe beam waist sizes and their position mismatches relative to the excitation beam using different settings of the probe beam telescope lens pairs by adjusting the separation distance of these lenses.

A combined result of all measurements is shown in a 3-D plot in Figure 4. For the first curve, designated by solid circles, the telescope magnification was changed in the range from ×1 to ×5, while the telescope lens distance for all magnification values was set to collimation. This curve is labeled "var" in Figures 4–6. For the second curve, designated by open circles and labeled "×1", we changed the distance between the paired lenses corresponding to ×1 magnification. The third curve (diamonds) and the fourth curve (squares) were obtained in the same manner, but with the "×2" and "×3" lens sets. For the variable describing the waist position mismatch, we chose the actual mismatch z_1 normalized by the Rayleigh range Z_R suggested by elementary TL theory.[21,22] Thus, four measurement sets map the TL signal along four paths in $w_p - z_1/Z_R$ space. These four paths can be more easily seen by looking at Figure 4's 3-D curves from the top, as is shown in Figure 5. Actual values of the TL signal in the entire range of parameter change can be better observed from the side of Figure 4, as presented in Figure 6. Figure 6 also displays the results of predictions of a thin lens mode mismatched TL model (solid lines), which we will discuss later in the text.

One striking feature of Figure 6 is that the experimental TL signal values for all four measurement curves group nicely

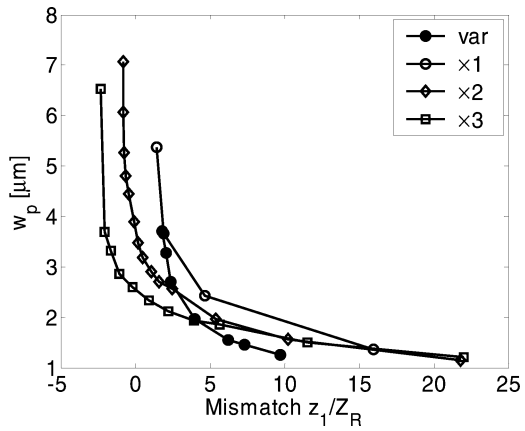

Figure 5. Top view of Figure 4. Probe beam waist size versus its mismatch to the excitation beam waist for all four data sets.

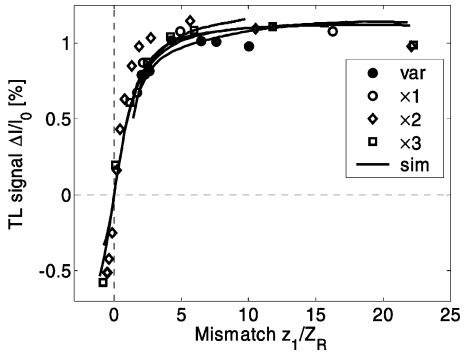

Figure 6. Side view of Figure 4, which presents the thermal lensing signal for all four data sets as a function of the probe beam waist position mismatch.

together, which means there is no significant difference of TL signal on the probe beam waist size, as long as we keep $w_p \geq w_e$. What matters most is the probe beam position mismatch z_1 expressed in Z_R units. We observe that the TL signal $\Delta I/I_0$ reaches its maximum value of 1.1×10^{-2} at $z_1 \approx 5Z_R$. Besides, the dependence on the mismatch is not very strong. The TL signal remains within 10% of its maximum value over a huge range, $2.5Z_R < w_1 < 22Z_R$. Such a small impact of the probe beam focusing parameters is a very good property for the device design because it reduces one possible source for measurement errors. Furthermore, the value of mismatch in this range will be obtained naturally with many singlet lenses thanks to chromatic aberration. For example, for an aspheric singlet C240TM-B that we used, the difference of focal lengths at 633 and 488 nm is equal to 0.136 mm and so is the distance between excitation and probe beam waist positions provided that both beams are collimated. As we can see from Figure 5, the waist position mismatch for collimated beams with w_p between 1.2 and 3.5 μm is in the range from $2.5Z_R$ to $10Z_R$. This gives a TL response close to its maximum value, as we can see in Figure 6.

Even though there is no theory for TL with tightly focused beams against which we can compare our results, it is quite interesting to see how far they are from predictions of "thin TL" theory, with full awareness that this theory is not applicable to our case. In the most detailed "thin TL" theory by Shen et al.,[22] the excitation and probe beam waists are mismatched both in size and in position. The size mismatch parameter is defined as $m = (w_{1p}/w_e)^2$, where w_{1p} is the probe beam size (radius) at the location

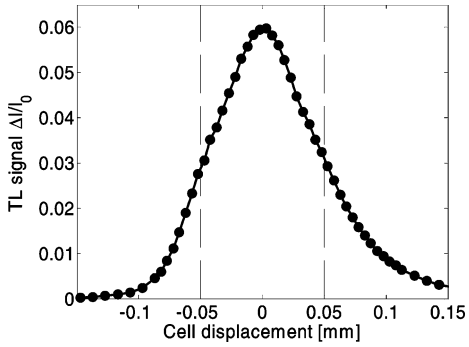

Figure 7. Thermal lensing signal as a function of cell displacement.

of the absorbing layer, whereas the position mismatch parameter is $V = z_1/Z_R$. Shen et al.'s expression for the absolute value of the TL signal for an excitation beam modulation period much longer than the temperature relaxation time of the medium, and for small TL signals, can be written as

$$\frac{I(t)}{I_0} = \theta \tan^{-1}\left(\frac{2mV}{[(1+2m)^2 + V^2](t_c/2t) + 1 + 2m + V^2}\right) \quad (1)$$

where $\theta = (P_e\, dn/dT)/k\lambda_p \alpha L$, P_e is excitation power, dn/dT is the temperature derivative of the refractive index of the medium, k is the thermal conductivity, α is the absorption coefficient, and L is the length of the absorbing layer. αL then is the fraction of the excitation power absorbed in the medium, and it is equal to that which could have been measured by ordinary UV–vis absorption. The factor in front of αL is a scaling coefficient between a TL measurement and an ordinary absorption measurement, and it is known as the "thermal lens enhancement factor". The parameter $t_c = w_e^2/4D$ in the first term of the denominator of this equation gives the time dependence of the probe beam intensity, and it is called a thermal time constant. D is the thermal diffusivity of the medium.

For $m = 1$ and $t \rightarrow \infty$, eq 1 has the same form as given by simpler "mode-matched" theory.[21] It predicts that the TL signal maximum will occur for the probe beam waist distance of $z_1 = \sqrt{3}Z_R$ from the thermally perturbed layer. For the mode mismatched case $m > 1$ and stationary thermal lens $t \rightarrow \infty$, eq 1 predicts that the TL signal increases and the optimum position mismatch z_1 shifts toward higher values. We should take into account, however, that with increasing mode mismatch parameter m the time needed to reach equilibrium rapidly increases. As a result, for fixed excitation beam modulation frequency and for high m values, the TL signal decreases.

With all this in mind, we calculated the waveforms of the TL signal for all pairs of w_e and z_1 in Figure 5 using eq 1 and our experimental parameters by taking $P_e = 28$ mW and the fraction of absorbed excitation power $\alpha L = 8.4 \times 10^{-4}$ for 5 μM quinizarin on the absorption path $L = 0.01$ cm. For the ratio $(dn/dT)/k$ and the thermal diffusivity constant for the mixture of 20% water and 80% methanol. we used linear interpolation.[25] The effective voltage amplitude of these waveforms at the first harmonics of the modulation frequency is plotted by solid lines in Figure 6. We can see that a thin lens theory predicts our results fairly well in

(25) Weimer, W.; Dovichi, N. J. *Appl. Phys.* **1986**, *59*, 225–230.

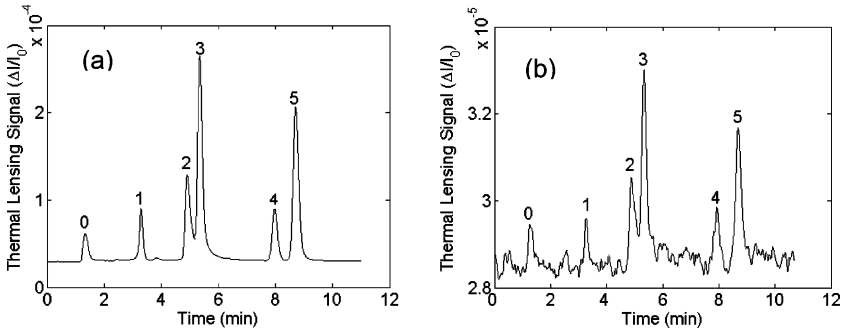

Figure 8. HPLC separation of (a) 1 μM and (b) 20 nM mixtures of five compounds with the 200-μm path-length flow cell using the coaxial thermal lens detection system. Peaks: (0) solvent front, (1) alizarin, (2) purpurin, (3) quinalizarin, (4) emodin, and (5) quinizarin.

the range of the mode position mismatch values $4Z_R < z_1 < 15Z_R$. The error of such a prediction is less than 10% in this entire range. We believe that the goodness of the approximation of using thin TL theory is one of the important results of this study.

We can draw several conclusions of rather general character about optimum conditions for TL measurement with tight focusing from the experimental results shown in Figure 6. First, we can see that most important is not the probe beam waist size itself, but rather the probe beam size in the region where the excitation beam is focused in the large range of the probe beam waist sizes, at least from $w_p = w_e$ to $w_p = 5w_e$. The second conclusion is that the TL signal can be predicted using eq 1 and our method of the waveform first harmonics calculation with an error smaller than 10% from known thermo-optical parameters of the solvent, and from the known fraction of the absorbed excitation beam power in the thin layer of liquid. The third conclusion is that the TL signal has a wide plateau for $4Z_R < z_1 < 15Z_R$, and within this area, the TL signal remains close to its maximum value. The fourth conclusion is that the required mode distance mismatch can be easily obtained using natural chromatic dispersion of singlet focusing lenses. We suggest that these conclusions provide practical guidelines for the design of a TL detector with tight focusing.

B. Analytical Volume Evaluation. If we examine Figure 5 and Figure 6, we can see that probe beam focusing parameters that bring us close to maximum TL efficiency are $w_e = 2$ μm and $z_1 = 5Z_R$. For these conditions, we recorded the TL signal as a function of the cell displacement in z-direction in order to determine the extent of the area near the excitation beam focus contributing to TL, and the result of this z-scan experiment is shown in Figure 7. The borders of our 0.1-mm-long cell are shown as vertical dashed lines. With the Rayleigh range of our excitation beam Z_{Re} equal to 12.3 μm, we might have expected a plateau in TL response with transient areas with the half-width of Z_{Re}. In contrast to these expectations, the transition area is much wider, and no plateau can be observed. This initially unexpected result means not only that a small volume of $\pm Z_{Re}$ from the focus is contributing to the TL signal but also that there is a quite significant contribution from the entire length of the cell. This conclusion may look less surprising if we notice that the diameter of the probe beam with the waist of 2 μm at the cell entrance is 28 μm, and at the cell exit it is still 13 μm, as it is focused at a distance from the cell center of $5Z_R = 95$ μm or beyond the cell limits. The excitation beam has a diameter of 2.4 μm in the middle of the cell, and this diameter increases to 10 μm at the cell borders. This means that if we consider the TL signal to be constructed from the cumulative layer-by-layer effect of thin lenses within the borders of the cell, and if we use eq 1 for evaluations, we must conclude that the contribution of the entire cell length still can be large because the m parameter remains larger than one.

In other words, we found out that even with tight focusing such that the Rayleigh range of the excitation beam is only a small fraction of the cell thickness, the thermal lens is still the result of its absorption over the entire length of the cell. This finding implies that evaluating the analytical volume as equal to the confocal volume, as has sometimes been done,[19] may in some cases lead to a significant underestimate of that volume, which causes an overestimate of the sensitivity. In our opinion, the entire probe beam volume contained within the cell should be used instead, which gives in our case the value of 0.033 nL.

C. Thermal Lensing Detection of the HPLC Separations. We applied the TL detector optimized as described in the previous section to HPLC separations using the same absorption cell and the same set of analytes as in previous CRDS work.[3] An example of HPLC separation of a mixture of five anthraquinone dyes each at 1 μM concentration detected by TL is shown in the left panel of Figure 8. The right panel shows the separation for the same dyes but for a 20 nM mixture. Direct comparison with Figure 6a from ref 3 gives us the value of the scaling coefficient from the TL signal to absorbance, and thus, we can determine the LOD in absorbance of our setup. The standard deviation of the baseline, or the baseline noise of the TL signal $\Delta I/I_0$, is 1.4×10^{-7}, which corresponds to 9.3×10^{-9} AU. The peak-to-peak noise of the TL signal baseline is 5.3×10^{-7}, corresponding to 3.5×10^{-8} AU. The signal-to-noise ratio for the smallest peak (peak 1, alizarin) for the 20 nM concentration is equal to 6, which gives a minimum detectable concentration (MDC) of 3.3 nM. For the 3.9 times stronger highest peak (quinalizarin), the MDC is 0.84 nM.

We also measured the HPLC calibration curves for the peak heights of each of the five substances in the concentration range of ~3.5 orders of magnitude from 0.02 to 100 μM for each component. These curves are shown in Figure 9. Each curve is linear and has an R^2 value of 0.999 except for quinalizarin. The curve for quinalizarin is linear up to 20 μM, but data points for 50 and 100 μM HPLC separation have smaller signals than expected. Among the five compounds, quinalizarin has the lowest solubility and precipitates very easily from the solution as the concentration is increased. Therefore, when the quinalizarin concentration is high, the actual concentration injected for HPLC separation is

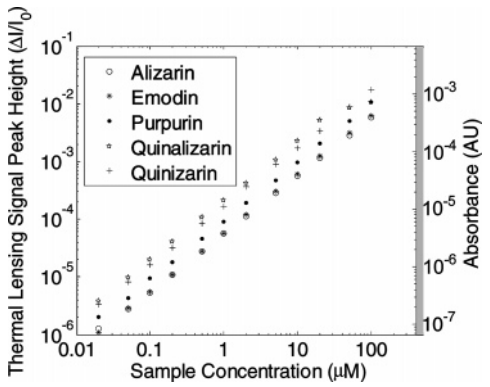

Figure 9. HPLC peak height calibration curves for each compound, which is pumped one at a time through the column.

lower than the marked concentration, resulting in a lower absorption value.

As a brief summary of presented HPLC results, we can conclude that TL demonstrated several times better performance than the previous CRDS detection study for HPLC separations. The peak-to-peak baseline noise of HPLC TL detection is 3.5×10^{-8} AU as compared with 2×10^{-7} AU achieved by CRDS detection.[3] The 140-fold baseline noise advantage of TL as compared with the peak-to-peak baseline noise of HPLC UV−vis (Shimadzu SPD10AV, $\pm 0.5 \times 10^{-5}$ AU, 1-s integration time) provides full compensation for its 50 times larger cell length of 10 mm and thus permits similar or better detection limits with tiny absorption cells only 0.2 mm long. Even though our absorption cell had large transverse dimensions, we expect that similar performance can be obtained with a much smaller detection area because both our pump beam and our probe beam diameter were no more than 120 μm at the cell entrance, and therefore, the cell volume can be as small as 3 nL, which opens the path to measurements without a penalty in limits of detection for nano-HPLC or CE applications. Finally, the TL HPLC detector developed in the present study demonstrated the dynamic range of 3.5 orders of magnitude in concentration and subnanomolar limits of detection.

DISCUSSION

Several previous studies have used TL as a detector of compounds separated by chromatography or electrophoresis. Excellent reviews of this work can by found in refs 11 and 20. Particularly notable examples include the detection[26] of amino acids tagged with 4-dimethylazobene-4-sulfonyl (DABSYL) chloride using a 458-nm argon ion laser line with a limit of detection of 180 nM and the detection of ferric ion using 1,10-phenanthroline[27] using the 364-nm line of the argon ion laser with a limit of detection of 36 nM. These studies were performed using a crossed-beam geometry, and this may explain why demonstrated detection limits were 1−2 orders of magnitude higher than in our work.

A coaxial beam thermal lens microscope has been developed by Kitamori and co-workers,[18,19] and single-molecule detection for strongly absorbing nonfluorescing dyes has been reported. They used a glass microchip 150 μm wide and 100 μm high and benzene as a solvent in order to maximize thermal lens response. The standard deviation in the baseline they achieved can be evaluated from the data in ref 19 as 1.3×10^{-8}AU with a 4-s averaging time, which is only a few times higher than the standard deviation of 9.3×10^{-9} AU with averaging time of 1 s reported in this work.

It appears that TL has reached maturity as a technique that is well suited for the detection of analytes in short-path-length devices at ultralow cell volumes with no penalty in minimum detectable concentration. However, almost all TL experiments of separated analytes have relied on visible excitation to cause absorption and heating whereas most compounds of interest absorb in the UV range. We suggest that TL will become widely adopted as a detector for chromatographic and electrophoretic separations only when it has been reduced to practice using suitable UV sources. We believe that compact, affordable sources of UV radiation will become available in the very near future, and thus, we believe that TL may become a detection method of choice.

CONCLUDING REMARKS

We developed an ultrasensitive optical absorbance detection system based upon coaxial thermal lensing that can work with subnanoliter volumes and 100-μm absorption path length. The standard deviation of baseline noise of 9.3×10^{-9} AU permits detection of analytes at subnanomolar concentrations and makes this system a viable detector for micro- and nano-HPLC as well as CE techniques. We performed a study of the influence of important design parameters on the detector performance. We also found out that the existing thin thermal lens theory can model the system response reasonably well, thus providing guidelines for the design of such systems. The developed detector has been applied to the HPLC separation of five anthraquinone dyes, and limits of detection below 1 nM have been achieved.

Received for review March 25, 2007. Accepted May 14, 2007.

AC0705925

(26) Seidel, B. S.; Faubel, W. *J. Chromatogr., A* **1998**, *817*, 223−226.
(27) Seidel, B. S.; Faubel, W.; Aiche, H. J. *J. Biomed. Opt.* **1997**, *2*, 326−331.